COMPOSITES & POLYCON 2009
American Composites Manufacturers Association
January 15-17, 2009
Tampa, FL USA

Design Optimization of GFRP Pole Structures Using Finite Element Analysis

by
Hamdy Mohamed, Department of Civil Engineering, University of Sherbrooke
Radhouane Masmoudi, Department of Civil Engineering, University of Sherbrooke

Abstract

The applications of the tapered glass fiber-reinforced polymer (GFRP) poles are started as an alternative for traditional materials such as wood, steel, and concrete, in overhead power line and distribution aerial network. This paper presents a finite element (FE) analysis of the nonlinear behavior of laterally loaded, full scale tapered GFRP pole structures. The FE model was used to detect the performance of GFRP poles having service opening (holes). Several FE simulations with different combinations of parameters such as fiber orientation, number of layers and thickness of layers were employed. Evaluation of the deflection and bending strength characteristics of GFRP Poles [20 and 33 ft] height are presented. Optimum new designs for three zones along the height of the GFRP poles are proposed, under equivalent wind load. The ultimate load carrying capacity and flexural stiffness are improved with a significant saving in the weight. The new designs are satisfied according to the allowable maximum deflection and the minimum ultimate moment capacity as specified in the ASTM, AASHTO LT S and ANSI standards.

Introduction

In recent years, FRP composites, which are made of reinforcing fibers and a thermosetting resin, have been widely used as advanced construction materials. FRP provide several advantages over traditional construction materials (steel, concrete, wood): high strength to weight ratio, high stiffness, resistance to corrosion, ease of installation and high durability [1]. Therefore, the tapered FRP poles are currently considered attractive in the application of the light poles and electrical transmission tower element.

There is a lack to study the behavior of the hollow tapered FRP pole structures. These due to the limited number of experimental and theoretical studies, which have been conducted on the behavior of the tapered GFRP poles structure under lateral load [2, 3, 4, 5 and 6]. Most of these studies were related to the behavior of the FRP poles without service opening. The existence of service opening in the FRP poles, reduce the strength at the location of this opening, due to small thickness-to-radius ratio, ovalization and local buckling behavior of the FRP poles [7, 8, 9 and 10]. Therefore the part which includes this hole must be addressed and finding the optimum geometrical details for it to be compatible with the upper and lower zones over the length of the pole, to attain the required total capacity under lateral loads.

The finite element analysis is a good way that can be used to simulate and predict the actual behavior of FRP poles. A theoretical analysis by finite element method were developed for the analysis of FRP hollow tapered poles, to perform a linear static analysis, linear buckling analysis, linear P-Δ analysis, a geometrical nonlinear analysis of beam-column-type bending and an ovalization analysis [2]. Extensive numerical results were presented showing the effect of different lamination and geometric parameters of the multilayered composite cylinder on the accuracy of the static and vibrational responses [11].

In this paper, the finite element program is used to perform a nonlinear numerical analysis for 20 and 33 ft tapered GFRP poles with service opening, under lateral load to present the wind load on the structure. A parametric study is carried out to study the effect of longitudinal and circumferential angle orientation of the fiber and wall thickness of three zones along the height of the pole. The ultimate capacity, top deflection and the ultimate moment capacity are presented to find the best optimum designs for the GFRP poles. Optimum new designs for three zones along the height of the GFRP poles are proposed, under equivalent wind load.

Geometrical Dimension of GFRP Poles

The first part in this study is the modeling by the finite element (FE) program of the GFRP poles [20 and 33ft] which were tested by [10]. Comparison between the FE and experimental results are presented. The second part is the optimization of the design of these two poles to meet the requirement for deflection and failure load. The specimens were tapered hollow sections, with different length. The inner diameters of the GFRP poles 20 ft at the base and at the top were 164.00 and 76.00 mm, respectively. The inner diameters of the GFRP poles 33 ft at the base and at the top were 261.00 and 114.00 mm, respectively. Each prototype is divided through the height into three zones, I, II and III as shown in Figure 1. The 101.6 x 304.8 mm-(width x length) service opening was located at the center of the middle zone II and was in

the compression side, when loaded. The stacking sequences at the three zones for [20 and 33 ft] GFRP poles are presented in Table 1.

Finite Element Model

In this study, an appropriate three-dimensional model is developed to accurately simulate the flexural behavior of GFRP pole structures; it is based on the finite-element software ADINA 8.4 [12]. Large deflection is included in the analysis and appropriate materials failure criteria (Tsai-Wu failure criterion) are used to determine the failure load. The results of the finite element analysis are verified through comparison with the available experimental data obtained from the static testing of full-scale prototypes [10], according to the recommendations described in ASTM and ANSI standards.

The following sections present the major features of the finite element method used in this study:

Geometrical Modeling

The 20 ft pole was modeled with total number of elements 1648 (16 and 103 in the circumference and longitudinal direction, respectively). In addition, the 33 ft pole was modeled with total number of elements 2224 (16 and 139 in the circumference and longitudinal direction, respectively). The mesh layout were fine in the bottom area of the maximum stress and expected failure zone, and gradually becomes coarse at the top, this was made by the automatic mesh density option of the program. The general layout of the mesh distribution and the used finite element models are shown in Figure 2.

The underground length of the GFRP poles were restraint along two opposite half circumference area, the first area at the end of the base and the second area at the ground line. Each node along the supported area was restrained against the vertical (in z-direction), the horizontal (in x and y directions) movements. This Configuration of restraints was to simulate the support condition described in standards [13, 14 and 15] for testing the Load- deflection behavior of FRP poles, see Figure 3.

Composite Shell Elements

An eight-node quadrilateral multilayered shell element was used in the model. Each node has six degrees of freedom, three translations (Ux, Uy, and Uz) and three rotations (Rx, Ry, and Rz). The composite shell elements are kinematically formulated in the same way as the single layer shell elements, but an arbitrary N number of layers can be used to make up the total thickness of the shell. The interfacial behavior between layers was considered full bonded. Layers are numbered in sequential order starting from 1 at the bottom of the shell [12].

Newton-Cotes with high order of 5×5 numerical integration was used for the evaluation of the element matrices in the r-s plane of the shell element, to avoid spurious zero energy. 3-point Newton-Cotes numerical integration was used through the shell thickness to obtain an accurate profile of the transverse shear stress.

The material model be used with the shell element is elastic-orthotropic with large displacement /small strain. In the large displacement formulation/small strain formulation, the displacement and rotation can be large, but the strains were assumed to be small. Orthotropic material properties in the fiber and transverse to the fiber direction were defined. Fiber orientation for each layer was specified by defining the fiber angle with respect to the element axes.

Loading

The FRP pole was subjected to a horizontal pressure load (W) below the top of the pole edge by 300 mm according to the ANS C 136.20-2005. The value of (W) was varied from zero to the ultimate load capacity corresponding to each pole. The pole was incrementally loaded using 100-150 time steps. This variation is automatically done by the ADINA User Interface (AUI) according to the condition of convergence. To avoid local failure under the applied load, the load had been distributed over circumferences area to simulate the same effect of the experimental load.

Material Properties

The material properties for both the fiber and the resin are presented in Table 2. The mechanical properties of the FRP laminate were obtained from the material properties of the E-glass fiber and the epoxy resin. They were used to calculate the effective modules of elasticity of the orthotropic material based on micromechanical models. The Rule of Mixture was used to evaluate the modulus of elasticity in the fiber direction (E_l), and the major Poisson's ratio (υ_{l2}) as follows [16]:

$$E_1 = E_f \mu_f + E_m \mu_m$$

$$\upsilon_{12} = \upsilon_f \mu_f + \upsilon_m \mu_m$$

Where,

μ_f and μ_m are the fiber and the matrix volume ratios, respectively;

E_f and E_m are the fiber and the matrix Young's modules, respectively; and

υ_f and υ_m are the fiber and the matrix Poisson's ratios respectively.

The equations given by [17] were used to calculate the effective Young's modulus in the transverse direction (E_2) and the shear modulus (G_{12}), by using the fiber and matrix properties, (E_2) and (G_{12}) were derived as follow:

$$E_2 = \frac{1}{\left[\frac{\mu_f}{E_f} + \frac{\mu_m}{E_m}\right]}$$

$$G_{12} = \frac{1}{\left[\frac{\mu_f}{G_f} + \frac{\mu_m}{G_m}\right]}$$

Where,

G_f and G_m are the fiber and the matrix shear modules, respectively.

Finite Element Results

The main objective of this section is to discuss the results of the finite element analysis. The numerical results in the current section are compared with the experimental results of [10] to assess the validity of the finite element analysis. Once the finite element was verified, it is extended to perform a more comprehensive parametric study. First we need to investigate what is the most convenient model with respect to mesh layout to simulate the FRP pole structure subjected to the top lateral load. The comparison was in terms of the load-deflection relationship and the ultimate load carrying capacity of the GFRP poles. Figure 4 represents the load deflection relationship for the experimental and finite element analysis for 20 and 33 ft height GFRP poles. It is evident from this figure that there is a strong correlation between the results obtained from the finite element analysis and the experimental results.

The Proposed Design of GFRP Poles

In this section, the objective is to obtain the best optimization with minimum weight for the complete details of the configuration for [20 and 33 ft] GFRP poles. This is to satisfy the requirement strength criteria for FRP poles which are given in ASTM, AASHTO and the general standard specification of the ANSI C136.20-2005 for the maximum deflection, ultimate load capacity and minimum embedment depth. The finite element method is employed to analyze the different proposed models for 20 and 33 ft GFRP poles. These models were proposed according to the survey in the literature review of experimental data from several sources [5, 6, 7, 8, 9 and 10] for different combination of parameters such as fiber orientation, number of longitudinal and circumferential layers, layer thickness and type of fiber. The details of the new proposed design are given in Tables 3 and 4 for 20 and 33 ft GFRP poles. It was assumed the number of layers is varied from 8 to 12, placed in two-layer-increment layers. All of these layers assumed that to be with longitudinal orientation except two circumferential layers for all zones I, II and III. The existence of service opining in zone II makes it weaker than the other zones. It is proposed to increase the main layers by three additional layers internally and externally in zone II, to make the total layers of this zone varied from 14 to 18. The fiber angles assumed to be +10°/-10° for longitudinal layers and 90° for circumferential layers, and 90°, +45°/-45° are used for the additional layers in zone II. The thickness of each layer varied from 0.28 mm to 0.50 mm and for the additional layers from 0.56 mm to 1.0 mm. Finally, a new fibers type of Linear mass (1100 g / km) and nominal yield (450 Yards / lb) are assumed as a reinforcement for the modeled GFRP poles.

Evaluation of Deflection and Bending Strength Characteristics for the New Proposed Design

All GFRP poles were analyzed using the developed finite element models; the thickness of each pole is computed using different load limit for each pole applied laterally at 12 inches below the top edge of the pole to attain the required strength criteria. This approach required that for each pole several trial sections were analyzed until the right thickness is achieved. Failure was defined either by material failure or by local buckling. The results indicate that a minimum thickness of a GFRP pole is achieved when using two circumferential layers with longitudinal layers from the total number of layers. The results of the finite element analysis for the new proposed configurations of the GFRP poles (20 and 33 ft) are given in Table 5.

The comparison between the maximum allowable deflection and the deflection of the new proposed design under an equivalent maximum wind loads is given in Table 6. Comparison between the ultimate moment capacity of GFRP poles of the new proposed design and the required ultimate moment capacity due to wind loads are given in Table 7.

For all GFRP poles (20 and 33 ft), it is clear that the deflection did not exceed the limit of maximum deflection under the equivalent wind load. The deflection is 25 % lower than the required deflection limit. The poles fail after reaching the specified minimum ultimate bending strength with factor of safety varied from 2.06 to 2.16. It means that an economic design for these GFRP pole is achieved with the new proposed design. From Table 8, it is clear that a significant saving in the weight is achieved with the new designs. All the details between the new and old designs for these GFRP poles, are the same except optimizing the number, thickness, fiber orientations and stacking sequence of layers.

Conclusions

The ultimate capacity and performance of the tapered filament wound GFRP poles (20 and 33 ft) subjected to cantilever bending are evaluated. The finite element analysis used in this study gives a good prediction of the flexural behaviours and failure loads. The proposed models with optimizing number, thickness, fiber orientations and stacking sequence of layers give excellent result. The internal and external additional three layers (90, ±45) for the laminate at the middle zone II with the service opening improved the flexural behaviour. Optimum cross-section dimensions for (20 and 33 ft) GFRP poles were obtained using the finite element models. These GFRP poles are designed to satisfy the requirement strength criteria as specified in the ASTM, AASHTO and ANSI standards for the maximum deflection and ultimate load capacity

Acknowledgments:

The research reported in this paper was partially sponsored by the Natural Sciences and Engineering Research Council of Canada (NSERC). The authors also acknowledge the contribution of the Canadian Foundation for Innovation (CFI) for the infrastructure used to conduct testing. Special thanks to the manufacturer (FRE Composites, St-André d'Argenteuil, Qc, Canada) for providing FRP tubes. The opinion and analysis presented in this paper are those of the authors. The technician Nicolas Simard participates in the specimen preparation and testing.

Author(s):

Hamdy Mohamed is a Ph.D. Candidate at the University of Sherbrooke, Sherbrooke, QC, Canada. He received his B.Sc. and M.Sc. degree from the Faculty of Engineering, Helwan University, Egypt in 1999 and 2005, respectively. His research interest is the use of fiber-reinforced polymers (FRP) in reinforced concrete structures. Mohamed is a member of several professional associations including the American Concrete Institute (ACI), the American Society of Civil Engineers (ASCE), the Canadian Society of Civil Engineering (CSCE) and the Egyptian Professional Engineers Association.

Email address:
Hamdy.Mohamed@usherbrooke.ca

Radhouane Masmoudi is a Professor at the University of Sherbrooke, Sherbrooke, QC, Canada. He received his M.Sc. and Ph.D. degree from University of Sherbrooke. His research interests include the development, design, testing and use of fiber-reinforced polymers (FRP) in utility and reinforced concrete structures as well as the finite element modeling of FRP structures. Masmoudi is a member of several professional associations including the American Concrete Institute (ACI), the Canadian Society of Civil Engineering (CSCE) and the Society for the Advancement of Material and Process Engineering (SAMPE).

Email address:
Rahouane.Masmoudi@usherbrooke.ca

References:

1. K. Fujikake, S. Mindess, and H. Xu, (2004). "Analytical Model for Concrete Confined with Fiber Reinforced Polymer Composite" JOURNAL OF COMPOSITES FOR CONSTRUCTION © ASCE, 8(4), 341-351.

2. ZM. Lin (1995). "Analysis of pole-type structures of fiber-reinforced Plastics by finite element method", Ph.D. Thesis, University of Manitoba, Winnipeg, Manitoba, Canada.

3. W. Crozier, J.P. Dussel, R. Bushey, J. West, (1995). "Evaluation of deflection and bending strength characteristics of fiber-reinforced plastic lighting standards". Department of Transportation, New York, State of California, USA.

4. G.L. Derrick (1996). "Fiberglass Composite Distribution and Transmission Poles", Manufactured Distribution and Transmission Pole Structures Workshop Proceeding, July 25-26, Eclectic Power Research Institute, 55-61.

5. S. Ibrahim, D. Polyzois, and S. Hassan (2000). "Development of glass fiber reinforced plastic poles for transmission and distribution lines". Can. J. Civ. Eng. 27, 850-858.

6. S. Ibrahim, and D. Polyzois (1999). "Ovalization analysis of fiber reinforced plastic poles". Composite Structures, 45, 7–12.

7. R. Masmoudi and H. Mohamed (2006). "Finite Element Modeling of FRP-Filament Winded Poles" Third International Conference on FRP Composites in Civil Engineering (CICE 2006), December, Miami, Florida, USA, 445-448.

8. H. Mohamed and R. Masmoudi "Behavioral Characteristics for FRP Composites Pole Structures: Nonlinear Finite Element Analysis", Proceedings of the Annual Conference of the Can. Soc. of Civ. Eng., Yellowknife, Northwest Territories, Canada..

9. R. Masmoudi, H. Mohamed and S. Metiche. (2008) Finite Element Modeling For Deflection and Bending Responses of GFRP Poles, Journal of Reinforced Plastics and Composites, Vol. 27, No. 6, 639-658.

10. S. Metiche and R. Masmoudi. (2007) "Full-Scale Flexural Testing on Fiber-Reinforced Polymer (FRP)

Poles", The Open Civil Engineering Journal, ISSN: 1874-1495, 1, 37-50, 2007.

11. K. Noor, W. Sctt Butron, . and M. Peters Jeanne. (1991) "Assessment of computational models for multi-layered composite cylinders" Int. J. solids structures. 27(10), 1269-1286.

12. ADINA. (2006). Theory Manual, version 8.4. ADINA R&D, Inc Wastertown, USA.

13. American Association of State Highway and Transportation Officials, AASHTO (2001), "Standard Specifications for Structural Supports for Highway Signs, Luminaires and Traffic signals".

14. American National Standard Institute. (2005). "Fiber-Reinforced Plastic (FRP) Lighting Poles, American National Standard for Roadway Lighting Equipment", USA, ANSI C 136.

15. American Society for Testing and Materials. (2001). "Standard Specification for Reinforced Thermosetting Plastic Poles", Annual book of ASTM Standards, D 4923 – 01, USA.

16. R.D Adams. (1987). "Damping properties analysis of composites" Engineering materials handbook. Edited by T.J. Reinhart et al. ASM International, Materials Park, Ohio, Vol. 1, Composites, 206–217.

17. D. Gay. (1989) Matériaux composites, Paris, 2e édition, Hermes. 485 p.

Table 1: Stacking sequences for the GFRP poles (Masmoudi et al 2008)

Pole **length**	20 ft	33ft
Zone I	[-60/60/-25/25/±70]	[70/-80/±20/70/-80]
Zone II	[90/-60/60/±15/±60]	[90/±15/70/-80]
Zone III	[±15/-60/70]	[±15/90]

Table 2: Mechanical and physical properties of fibers and resin

	Fibers (E-Glass)
Linear mass (g / km)	2000
Nominal Yield (Yards / lb)	250
Tensile modulus(MPa)	80 000
Shear modulus(Mpa)	30 000
Poisson's ratio	0.25
	Epoxy resin Araldite GY 6010
Density (Kg / m3)	1200
Tensile modulus(Mpa)	3380
Shear modulus(Mpa)	1600
Poisson's ratio	0.4

Table 3: New design stacking sequences for the GFRP poles

Pole length	***Zone I and III*** (M-L)	***Zone II*** {A-L, [M-L], A-L}
20	*[90, $(\pm 10)_3$, 90]*	*{90, ±45, [90, $(\pm 10)_3$, 90] ±45, 90}*
33	*[90, $(\pm 10)_4$, 90]*	*{90, ±45, [90, $(\pm 10)_4$, 90] ±45, 90}*

M-L : Main layers
A-L : Additional layers

Table 4: Details of new design Laminate for the GFRP poles

Proto. length	*Zone I, III*			*Zone II*					
	N_T	*Thick-ness of each layer* (M-L) *(mm)*	T_T *(mm)*	N_T	*No. of main layers* (M-L)	*No. of addi-tional Layers (M-L)*	*Thick-ness of each layer (M-L) (mm)*	*Thick-ness of each layer (A-L) (mm)*	T_T *(mm)*
20	*8*	*0.28*	*2.24*	*14*	*8*	*6*	*0.28*	*0.56*	*5.60*
33	*10*	*0.35*	*3.50*	*16*	*10*	*6*	*0.35*	*0.70*	*7.70*

N_T : Total number of layers
T_T : Total thickness

Table 5: Results of finite element analysis for the new design

Proto. length	$P_{F.E}$ (N)	Maximum deflection (mm)	Weight (kg)
20	1560	730	15.77
33	2930	1343	58.70

$P_{F.E}$: Finite element failure load

Table 6: Comparison between the maximum allowable deflection and the deflection of the new proposed design for the GFRP poles under the equivalent maximum wind loads.

Proto. length	$\Delta_{F.E}$ (mm)	Δ^* (mm)	$\Delta_{F.E}/\Delta^*$	Notes
20	338.6	457.2	**0.75**	**Safe**
33	652.9	853.4	**0.76**	**Safe**

$\Delta_{F.E}$: Deflection of finite element analysis under the equivalent maximum wind loads.
Δ^* **:** The maximum allowable deflection under the maximum wind loads (10 percent of the pole length above the grade line).

Table 7: Comparison between the ultimate moment capacity for GFRP poles of the new proposed design and required ultimate moment capacity due to wind loads.

Proto. length	$P_{F.E}$ (N)	$M_{F.E}$ (N.m)	M_w (N.m)	Factor of safety $M_{F.E}/M_w$	Notes	Weight (kg)
20	1560	6864	3168	**2.16**	**economic design**	15.77
33	2930	24026	11620	**2.06**	**economic design**	58.70

$M_{F.E}$: Ground moment due to finite element failure load
M_w : Combined ground moment due to wind loads on luminaire and pole

Table 8: Factor of safety for moment, deflection and the weight ratio of [10] and proposed GFRP poles.

Pole length	Factor of safety for moment		Factor of safety for deflection		Weight ratio	Reduction in weight
	M_{test}/M_w	$M_{F.E}/M_w$	Δ_{test}/Δ^*	$\Delta_{F.E}/\Delta^*$	W_{test}/W_{prop}	%
20	2.44 Uneconomic	2.16 safe	1.18 unsafe	0.75 safe	1.347	**29**
33	3.14 Uneconomic	2.06 safe	0.81 safe	0.76 safe	1.40	**28**

Δ_{test} **:** Deflection test under the equivalent maximum wind loads.

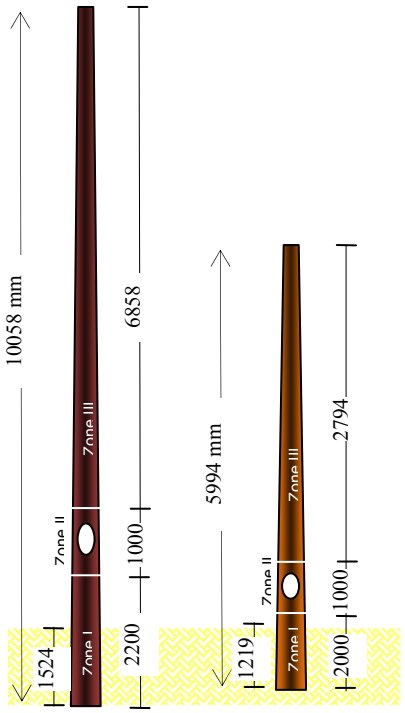

33 ft **20 ft**

Figure 1: Poles dimension

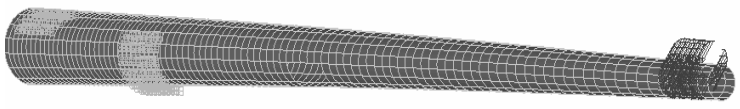

Figure 2: Finite element mesh

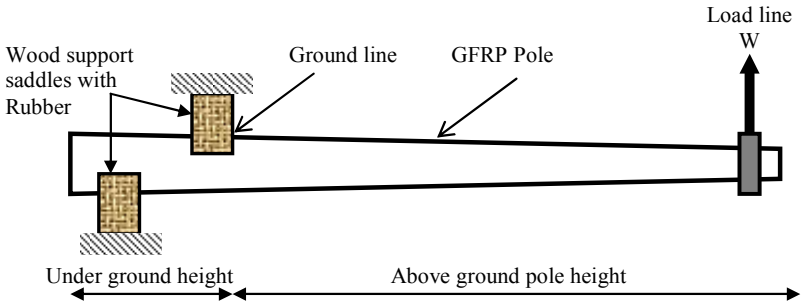

Figure 3: Specified methods for testing FRP poles

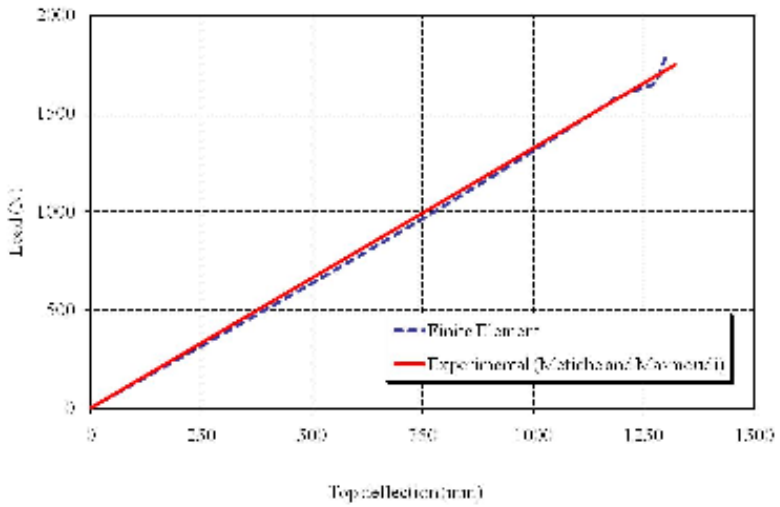

Figure: 4.a. Comparison between experimental and FE load-deflection relationship for 20 ft GFRP pole

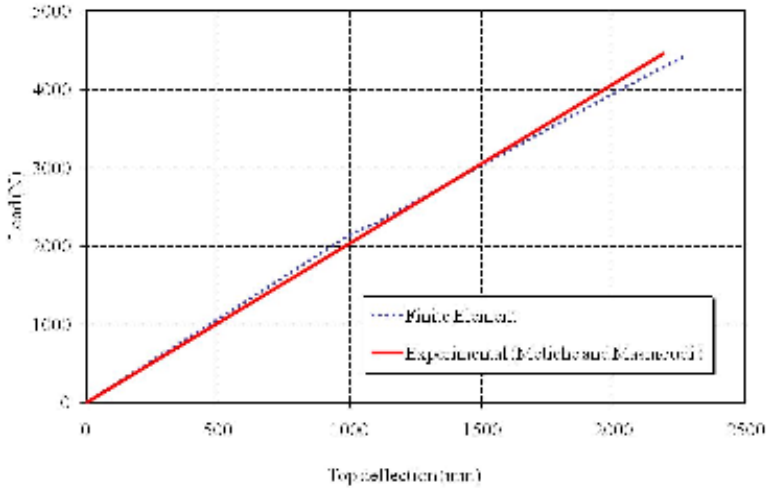

Figure: 4.b. Comparison between experimental and FE load-deflection relationship for 33 ft GFRP pole